17

Multigluon emission, the dipole cascade model and other coherent cascade models

17.1 Introduction

In the last chapter we considered the bremsstrahlung cross section for dipole radiation. This cross section is valid even for multiple QED bremsstrahlung. But there is a major difference between an abelian and a nonabelian gauge field theory in connection with multiquantum radiation.

For an abelian gauge theory, like QED, the emitted quanta are chargeless. Therefore the current is the same before and after the radiation (besides the recoils, which pose particular problems in all theories).

For QCD, the emission of (the color-8 charged) bremsstrahlung gluons may actually be disastrous. The original current in e.g. an e^+e^- annihilation event consists of a color-3 and a color-$\bar{3}$ charge (the original $q\bar{q}$-pair), forming the primary dipole. But after the emission of a gluon the current consists of a state with color-$(3, 8, \bar{3})$ charges moving in different directions. It is a great simplification that *the three charges to a very good approximation can be tretaed as two independent dipoles* [27].

We will start by presenting this result and then continue the discussion in terms of the *Lund dipole cascade model*, the DCM [75]. In this model the production of new gluons stems at every step from the formation of dipoles by pairs of previously emitted partons, and the process leads to new and smaller dipoles. The coherence conditions can in a simple way be realised in the DCM. The process is implemented in a Monte Carlo program, ARIADNE [92]. Within the DCM it is also easy to clarify the way the directrix of the final-state string emerges. We will show that the coherence conditions of multigluon emission in this model tend to bend the directrix in a characteristic way towards an ever smoother curve.

After that we will turn to the description of models in which the subsequent gluon radiation is related to a single one of the already existing partons. It is then necessary to partition the dipole cross section

https://doi.org/10.1017/9781009401296.017 Published online by Cambridge University Press

in a consistent way into the contributions from the two charges at the endpoints. It is necessary to take coherence into account by means of the strong angular ordering condition derived in Chapter 16.

We will also be more precise with respect to the polarisation correlations. We will exhibit the so-called splitting functions, which correspond to approximations to the dipole emission formulas valid when the radiated gluon is collinear to one of the charges.

We briefly describe the procedures in two Monte Carlo models of this kind, HERWIG, [94], and JETSET, [105]. At the same time we consider some features of the Webber fragmentation model. We will also discuss the *gluon splitting process.* In particular we exhibit *the results of a competition between different stochastic processes*, in this case gluon emission, $g \to gg$, and gluon splitting, $g \to q\bar{q}$.

We do not know the higher-order perturbative results for the cross sections. Therefore there is a problem in connection with how to partition the recoils in the emissions. We will show that within the DCM the results are stable and consistent.

There is actually a particularly nice relationship between the DCM and the Lund fragmentation model. It turns out that the dipoles of the DCM occur just in the regions where the Lund model would span a string. *Consequently all 'new' gluon emissions, with ensuing activity, occur where the Lund model already provides for particle production.*

In other words the DCM (and models containing a correct treatment of the coherence conditions) provide for gluon production in accordance with the string effect, discussed in Chapter 15. The softer gluon radiation (softer because the corresponding dipole masses in general are smaller) in the string regions only serves to provide smaller gluon excitations on an already existing string.

The result is that *there is a moving interface between the radiation of more and softer gluons and the fragmentation process of the Lund model.* We will exhibit this property and discuss the consequences in some detail.

The reason that the Lund model results and the results of the Webber-Marchesini model [94] agree so well, despite the large conceptual differences in the models, is that both models implement the bremsstrahlung coherence conditions. In other words *both models contain* (in a statistical sense) *activity inside the same regions of phase space.*

17.2 The consequences of the second-order matrix element

The main difference between QED emission of photons and QCD emission of gluons is the final-state current distribution. In the QED case the γ's are chargeless and apart from the recoil problems the original current

https://doi.org/10.1017/9781009401296.017 Published online by Cambridge University Press

is still the same. In QCD, however, we start with a color-$3\bar{3}$ dipole and afterwards end up with a $(3, 8, \bar{3})$-charge situation.

There is, however, one simplification. We started out with a color singlet composed of the 3- and $3\bar{3}$-charges and it is evident that the three charges $(3, 8, \bar{3})$ must also together form a color singlet. Therefore in particular the combined qg-charge must compensate the $\bar{q}$-charge and similarly the combined $g\bar{q}$-charge must compensate the q-charge. Such a charge situation may have implied the occurrence of higher multipole charge distributions. However, *up to a small correction we only obtain two new dipole emitters.* We will now treat the radiation of one more gluon along these lines.

The cross section for the process $e^+e^- \to qg_1g_2\bar{q}$ has been calculated in great detail and the full expression, [56], is very long and rather complicated. If we assume that the cms energies of the particles are strongly ordered, i.e. $E_2 \ll E_1 \ll E_q, E_{\bar{q}}$ then it is much simplified. The total angular distribution is then a product of two expressions, [27], where we make use of the antenna pattern distribution W defined in Eq. (16.46). The factor N_c is the number of colors and is proportional to

$$W_{q,\bar{q}}(\mathbf{n}_1) \times \left[W_{q,1}(\mathbf{n}_2) + W_{1,\bar{q}}(\mathbf{n}_2) - \frac{W_{q,\bar{q}}(\mathbf{n}_2)}{N_c^2} \right] \tag{17.1}$$

Therefore in this limit we can regard the process as if

- there is a first emission of g_1 from the original $q\bar{q}$-dipole,
- then there is a second emission of g_2 either from the qg_1-dipole or from the $g_1\bar{q}$-dipole. *The two dipoles in this way work independently.*
- the third term in the brackets is small and may be neglected

The dipole cascade model

In this model, [75], the pattern exhibited in Eq. (17.1) is taken all the way. Thus, the radiation of two gluons produces three dipoles and then these new dipoles are allowed again to decay independently. At each step there is a new gluon emitted and the corresponding dipole is then subdivided into two. After n gluon emissions there are then $n+1$ dipoles.

The cross sections used in the Monte Carlo simulation program ARIADNE [92], which implements the model, are

$$\begin{aligned} dn_{q\bar{q}\to qg\bar{q}} &= \frac{2\alpha_s}{3\pi} \frac{(x_1^2 + x_3^2)dx_1dx_3}{(1-x_1)(1-x_3)} \\ dn_{qg\to qgg} &= \frac{3\alpha_s}{4\pi} \frac{(x_1^3 + x_3^2)dx_1dx_3}{(1-x_1)(1-x_3)} \\ dn_{gg\to ggg} &= \frac{3\alpha_s}{4\pi} \frac{(x_1^3 + x_3^3)dx_1dx_3}{(1-x_1)(1-x_3)} \end{aligned} \tag{17.2}$$

https://doi.org/10.1017/9781009401296.017 Published online by Cambridge University Press

We will come back later to the powers in the polarisation sum in the numerators. Note that if a g is the emitter then there is a power 3 for the corresponding variable. For a q- or $\overline{q}$-emitter there is a power 2.

The color factors in the cross sections are also different. There is no suppression if a gluon splits up into two gluons. If a q and a $\overline{q}$ in a pair are the emitters there is (cf. Chapter 4) one chance in nine of obtaining a color singlet combination. Therefore only 8/9 of the color combinations are gluons, which is just the ratio between the color factors in Eq. (17.2).

We will from now on use the variables $k_\perp, y$ defined in Eq. (16.39) of Chapter 16. In particular the stochastic process of multigluon radiation in ARIADNE uses the transverse momentum variable $k_\perp$ as the *ordering variable*. We will start by clarifying the meaning of this notion.

17.3 An aside on ordering and the Sudakov form factors

A stochastic process is always defined by means of a direction. In order not to double-count the contributions they must be organised according to some system, so that we have the first step, the second etc. In the Lund fragmentation model the process is e.g. ordered along the lightcone(s) (the equivalence of the orderings actually provides a unique process, cf. Chapters 7–9). For multigluon emission processes the model builders use different ordering variables but the choices are in general made so as to account for the coherence conditions of the radiation.

If the available phase-space cells are subdivided and numbered according to the prescribed ordering variable, each with a given probability a_k that an event should happen, *then the very first event is defined by the requirement that it happens in the cell j with probability $P^{(1)}(j)$, where*

$$P^{(1)}(j) = a_j \prod_{k=1}^{j-1} (1 - a_k) \tag{17.3}$$

The product corresponds to the requirement that nothing has happened in the first $j-1$ cells.

In the limit when the subdivision of phase space becomes more and more fine-grained and the number of cells grows correspondingly we obtain

$$dP(A) = dn_g(A) \exp\left(-\int_\Omega dn_g\right) \tag{17.4}$$

This is the probability that no emission has occurred in the region Ω and one emission occurs at the boundary point A. The exponential factor in Eq. (17.4) is usually referred to as a *Sudakov factor* [107]. It is of course

https://doi.org/10.1017/9781009401296.017 Published online by Cambridge University Press

also the factor occurring in decay formulas generally (cf. the description of the Artru-Menessier-Bowler model in Chapter 8 for a different context).

We have in this way made use of general probability concepts. The properties of the Sudakov factor are governed by the density dn_g. It may happen that dn_g is not a local quantity independent of the prehistory, i.e. the path from the starting point to A. Then the integral must be correspondingly 'path-ordered'. In the DCM where the gluon emissions are $k_\perp$-ordered the integral is over the values of $k_\perp \geq k_{\perp A}$ and dn_g is given by the relevant formula in Eq. (17.2). As we will see later on there are also other ways to order a QCD perturbative parton cascade, still keeping to the coherence conditions. The coherence conditions in QED photon emission are simpler. One may generally choose any ordering in the phase space which is defined by the properties of the charged current.

Actually it was for multiple photon emissions in QED that Sudakov first constructed the form factor. His arguments were, however, not based upon probabilities. He pointed out that if we consider the emission of a fixed (*exclusive*) multiphoton state then there are many Feynman diagrams contributing to the matrix element. In particular at every new order in the coupling constant there are virtual corrections, corresponding to emission and reabsorption of photons in the available phase space. He was able to calculate the leading contributions from this series, i.e. those with the largest energy dependence, and *it turned out that the resulting sum 'exponentiated' into just the form factor in Eq. (17.4).*

In this way the probability of emitting nothing is directly in perturbative field theory related to the 'virtual corrections' from emitting and absorbing anything else besides the exclusive state. The 'real' emission density dn_g is then the same as the virtual emission-reabsorption density!

This result is also reasonable from Eq. (17.4). We may imagine that there is a small region $\delta\Omega$ in Ω around the boundary point A. If we allow for emission of anything inside $\delta\Omega$ but neglect to observe the results then we go over to an inclusive distribution: we observe that there is nothing in $\Omega - \delta\Omega$, there is something at the boundary point and there may be anything in $\delta\Omega$. The probability for this is given by Eq. (17.4) with $\Omega \to \Omega - \delta\Omega$. *Therefore summing up contributions in a region means that the region vanishes from the Sudakov factor*!

We will meet this situation again in a somewhat different context in connection with deep inelastic scattering (DIS) in Chapters 19–20. We would then like to subdivide the total radiation in a state into two sets. One of these corresponds to the production of a state with a well-defined set of gluons, usually referred to as the initial-state bremsstrahlung (ISB). In the linked dipole chain model these gluons correspond to a set of connected dipoles. The other set, the final-state bremsstrahlung, (FSB) corresponds to the available radiation from these dipoles. Then we may

sum up the FSB contributions to the Sudakov factor when we calculate the contribution from the ISB to the cross section.

But for every exclusive state there is, of course, a Sudakov factor for that particular FSB emission from the ISB dipoles. Taking all the states into consideration, however, they do sum up to a factor 1 in the cross section.

17.4 The generalisation of the λ-measure to multigluon situations

In section 15.7 we have introduced a generalised rapidity variable called λ that has the same properties for an event containing a hard gluon emission as the ordinary rapidity variable has for two-jet events, i.e. those events that correspond to the fragmentation of a straight $q\bar{q}$-string.

Based upon the properties of multigluon emission as it is described above in the dipole cascade model we will now generalise the definition of the λ-measure to multigluon emission. There are two major properties of the cascade and the fragmentation processes that we need.

Firstly we note that according to the perturbative dipole cascade model each dipole may during the cascade be subdivided into two new dipoles by the emission of a gluon. While the original dipole moves as a straight string segment between the two light rays of the endpoint partons the two 'new' dipoles will move apart as string segments spanned between each of the original endpoints and the gluon. In this way the dipoles correspond to color-field *links* between the *corners* defined by the partons. The new dipoles will move apart so that the fields are stretched over the gluon light ray (we use the same notions as in the description of the string surface in space-time in Chapter 15). An example is given by Fig. 15.9 in which a state containing a q, two g's and a $\bar{q}$ (they will be indexed $1, 2, 3, 4$, respectively) is shown as it develops in space-time.

Secondly, after the emission of the two gluons there are three lightcone regions spanned between the q_1 and the g_2, between the g_2 and the g_3 and between the g_3 and the $\bar{q}_4$. Inside each lightcone region there will be a typical hyperbola decay during the fragmentation process as we have described before (see Chapters 9 and 15). Thus the final-state particles are on the average produced along a hyperbola with a fixed proper time with respect to the origin. There may also be a few particles produced around the gluon corners, i.e inside the gluon fragmentation regions (see Fig. 17.1).

It is then evident how to generalise the λ-measure. The result in Eq. (15.26) that the total available region for particle emission is changed from the straight, string fragmentation result $\Delta y = \log(s/s_0)$ to $\lambda =$

https://doi.org/10.1017/9781009401296.017 Published online by Cambridge University Press

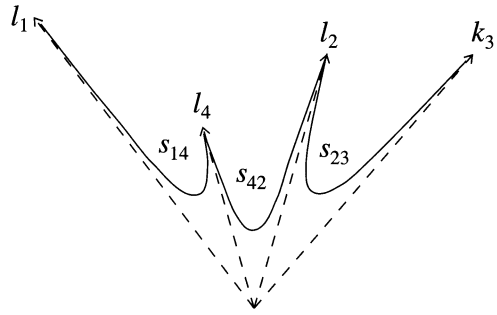

Fig. 17.1. The situation after the appearance of a second gluon. Note the two 'tips' dragging out hyperbolas around the gluon corners, which each contain a number of particles proportional to the value of $\log k_\perp^2$ for the gluon in question.

$\log(s/s_0) + \log(k_\perp^2/s_0)$, will be further changed to

$$\lambda = \log(s_{12}/s_0) + \log(s_{23}/s_0) + \log(s_{34}/s_) \tag{17.5}$$

i.e. into the hyperbolic size of each of the three lightcone sections. In Eq. (17.5) we have used the same scale variable s_0 whether it is a gluon or a quark fragmentation region (cf. the discussion in subsection 15.6.4).

According to the dipole cascade model we may consider the size of λ as emerging in a step-by-step process in which we first have the original dipole $q\bar{q}$ (total energy-momentum P_{tot}) changing into e.g. $q_1 g_2' \bar{q}_4'$ (with energy-momenta k_1, k_2', k_4') and finally into $q_1 g_2 g_3 \bar{q}_4$ (with energy-momenta l_1, l_2, l_3, l_4). (The primed variables are introduced to indicate that in the last emission, which in this case according to the dipole cascade model corresponds to emitting the g_3 from the dipole $g_2' \bar{q}_4'$, there will be recoil changes in the emitters' energy-momenta). Energy-momentum conservation implies

$$P_{tot} = k_1 + k_2' + k_4' = l_1 + l_2 + l_3 + l_4 \tag{17.6}$$

and the independence of the emission according to the dipole cascade model implies that $k_1 = l_1$. Therefore $k_2' + k_4' = l_2 + l_3 + l_4$. Consequently the first gluon is emitted at an invariant $k_{\perp 2}^2 = s_{12}' s_{24}'/s$ and the second at an invariant $k_{\perp 3}^2 = s_{23} s_{34}/s_{234}$ where $s_{234} \equiv s_{24}'$ in easily understood notation.

The result in Eq. (17.5) can then be reformulated in the following way:

$$\lambda \simeq \log s + \log(s_{12} s_{234}/s) + \log(s_{23} s_{34}/s_{234}) \equiv \log s + \sum_{j=2}^{3} \log k_{\perp j}^2 \tag{17.7}$$

where we have approximated s_{12} by s_{12}', thereby neglecting the recoil of the gluon emitter 2 in the second emission.

https://doi.org/10.1017/9781009401296.017 Published online by Cambridge University Press

Equations (17.5) and (17.7) can evidently be generalised into multigluon situations and are well defined as long as all the squared masses $s_{i,i+1}$ of two color-connected gluons are larger than the scale s_0. We will later extend the definition in an infrared-stable way.

Finally it is also obvious that the measure λ defined above corresponds to the total generalised rapidity region available for final-state hadron emission, i.e. it could have been called $\Delta\lambda$ in the same way as we introduced $\Delta y = \log(s/s_0)$ for the two-jet events. When we extend the definition of λ in section 18.7 it is possible to define a local value $\lambda(\sigma)$ where σ parametrises the points along the directrix of the state (cf. the general description of string motion in terms of the directrix in Chapter 15). Every point along the hyperbolas spanned between the color-connected gluons will then have a well-defined value of $\lambda(\sigma)$ between $\lambda(0) = 0$ and $\lambda(E/\kappa) = \lambda$.

17.5 The phase-space triangles of DCM

We will next discuss the available phase space. The subdivision of the very first dipole by the radiation of a gluon with $k_{\perp 1}$ and y_1 will in accordance with Eqs. (16.39) lead to a splitting of the original mass-square s into the two dipole mass-squares

$$s_{12} = k_{\perp 1}\sqrt{s}\exp y_1, \quad s_{23} = k_{\perp 1}\sqrt{s}\exp(-y_1) \tag{17.8}$$

Thus, in the phase space approximately described by the triangular region in Fig. 16.4 there is one point shown in Fig. 17.2 corresponding to the $(k_{\perp 1}, y_1)$-variables of the first emission. The region above this point, i.e. the triangle above the hatched line, does not contain any gluons. If this is the first emission the region Ω in Eq. (17.4) is just this triangle according to the ordering in ARIADNE.

We next construct the phase space for the 2nd emission. The logarithm of the squared masses in Eq. (17.8) can be described in size according to Fig. 17.2. Thus

$$\begin{aligned} L_{12} &\equiv \log(s_{12}/s_0) = (\kappa_1 + L)/2 + y_1 \\ L_{23} &\equiv \log(s_{23}/s_0) = (\kappa_1 + L)/2 - y_1 \end{aligned} \tag{17.9}$$

where we have introduced the variables from Eq. (16.42). In the figure, starting from the emission point, we have drawn out a triangular fold, which sticks out of the earlier triangle. The length of each triangular side of the fold baseline is $\kappa_1/2$ and the triangular height is of course κ_1. Therefore the distances from the lower left and lower right corners of the original triangle along its baseline to the tip of the fold are

$$\frac{L}{2} + y_1 + \frac{\kappa_1}{2} = L_{12}, \quad L_{23} = \frac{L}{2} - y_1 + \frac{\kappa_1}{2} \tag{17.10}$$

https://doi.org/10.1017/9781009401296.017 Published online by Cambridge University Press

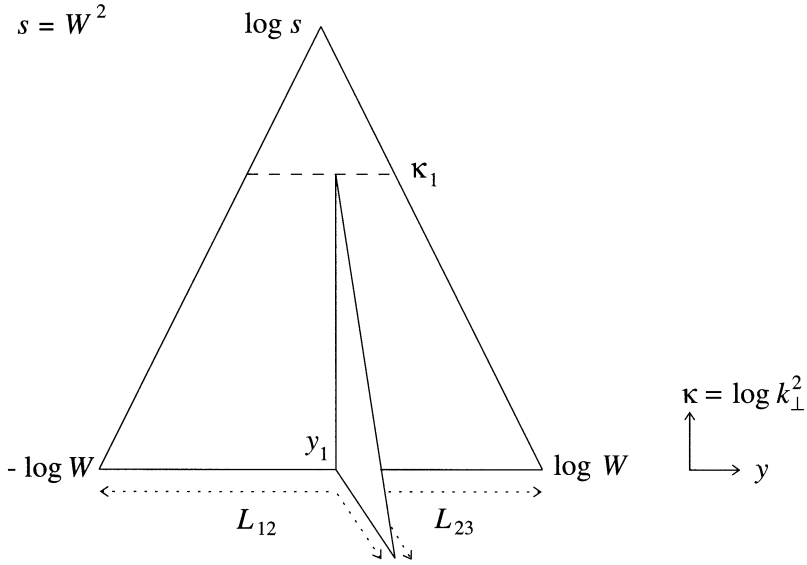

Fig. 17.2. The production of two new dipoles, by the emission of a gluon with $k_{\perp 1}, y_1$ described in the logarithmic phase-space variables κ, y. The (logarithmic) size of the dipoles is indicated along the baseline and out to the tips of the added triangular fold.

respectively. The folded triangle is the increase in phase space in QCD for further gluon emissions, given the variables of the first emission. It was introduced as the generalised rapidity variable λ in Chapter 15. The length of the baseline (including the triangular fold) is evidently $\lambda = L + \kappa_1$, i.e. that obtained in Eq. (15.27).

At this place we make the following further comment:

- if we use another scaling variable s_1 instead of s_0 in the definition of κ then each triangular construction is lengthened or shortened by the factor $\log(s_1/s_0)$. Each dipole size is changed and therefore the sum of the two dipole lengths is changed correspondingly.

In particular if we use the scale $s_1 = k_{\perp 1}^2$ then the baseline changes to the size $L - \kappa_1$. This is the rapidity region available for the first radiation. In Chapter 18 and also in Chapter 20 we will consider κ_1 as the (logarithmic) 'virtuality' of the dipole and then $L - \kappa_1$ is the size of the dipole just before it decays.

The phase-space triangle (before the second emission) has been changed into two cutoff triangles, corresponding to the two new dipoles and one

https://doi.org/10.1017/9781009401296.017 Published online by Cambridge University Press

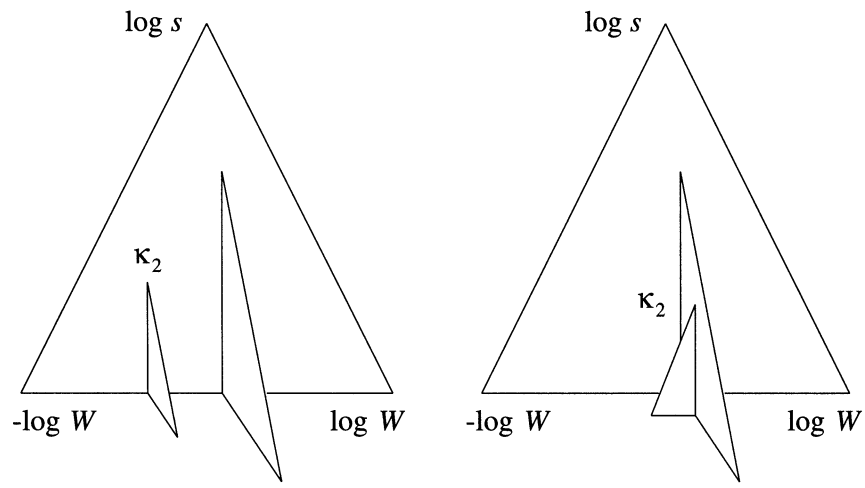

Fig. 17.3. The second emission in the cascade corresponds to one more projecting fold. The two cases corresponding to (*a*) and (*b*) are discussed in the text.

empty part (note that the next emission must be below κ_1), as follows. We have

1 one triangle above κ_1 in which there are no gluons;

2 one left (cutoff) triangle corresponding to the new dipole qg with mass s_{12} (to see this triangle imagine that you bring the fold towards the right in Fig. 17.2 into the old triangle);

3 one (also cutoff) triangle corresponding to the new dipole $g\overline{q}$ with mass s_{23} (bring the fold towards the left in Fig. 17.2 into the old triangle).

We may now repeat the whole process, moving downwards towards smaller κ in each of the two triangles, until somewhere we find the next emission, (κ_2, y_2). This new radiation may then occur in any one of the two independent dipoles.

In Fig. 17.3(*a*) we have divided the dipole s_{12} and added a new fold which at the baseline has the (double-sided) size κ_2. In Fig. 17.3(*b*) the corresponding division occurs in the folded triangle stemming from the first emission. This construction warrants further comments. In principle we could say that the situation described in Fig. 17.3(*b*) corresponds to

https://doi.org/10.1017/9781009401296.017 Published online by Cambridge University Press

the emission of a gluon 'collinear' to the first gluon. We would then define a collinear gluon as one having a y-difference variable measured to the end of the dipole smaller than the original $\kappa_1/2 = \log(k_{\perp 1}/\sqrt{s_0})$.

But for independent dipoles such a statement would be rather arbitrary. A little reflection tells us that the crucial variable for 'collinearity' is the difference between the emission point and the point closest to it along the edge of the triangular fold.

We will find in Chapter 18 that there is actually a scale at the endpoint of the dipoles. Closer to the endpoint than this scale we in general get into trouble, because of the kinematics of the recoils, in defining the real direction of the partons after any emission. This scale is to a good approximation independent of the earlier emissions.

The same construction can now be used when we continue towards smaller and smaller κ-values and correspondingly smaller dipole masses. Every radiation of a new gluon corresponds to a new fold in the triangle. We will return to this picture in the next chapter. There are two further comments on the construction of the triangular phase space with its many folds.

Firstly in Chapter 15 we have shown the string space-time surface when there are several gluons radiated. The measure λ was then described as the length of a set of hyperbolas spanned between the gluon peaks. These hyperbolas correspond in the phase-space triangle to the straight lines between the peaks of the projecting triangles and the folds themselves correspond to the gluons.

Secondly the variables used in the triangular phase space are the invariants $k_\perp, y$. It may be dangerous to associate these variables with the 'true' transverse momenta and rapidities with respect to a physical axis in the event. The invariant variables have a meaning in each dipole's rest frame. This means that the size and the place of the phase-space folds depend upon the earlier emissions.

17.6 The description of multigluon emission as a process on the directrix

1 The process

We will in this section demonstrate the way the directrix is gradually changing during the radiation cascade of gluons. The directrix is in Chapter 15 defined as the connected curve obtained when the parton energy-momentum vectors are laid out in color order.

We will only consider the space parts of the directrix in this section and only the first half-cycle of the curve. The second half is the same but with the parton energy-momenta laid out in the opposite order, according to the prescriptions for the directrix of a string starting at a single point.

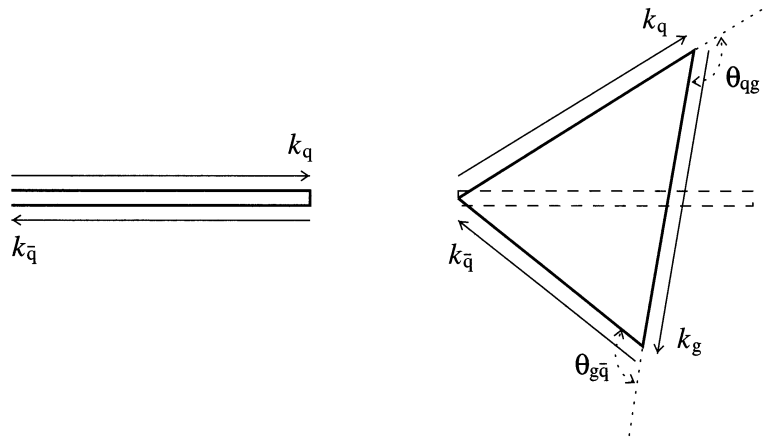

Fig. 17.4. The $q\bar{q}$-state directrix and the triangular directrix after the first gluon emission.

The directrix corresponding to the original $q\bar{q}$-state is in the cms just a double line, each part having length $W/2$ with W the cms energy of the state (see Fig. 17.4). The first gluon emission changes the double line into a triangle with the sides corresponding in turn to the q-momentum, $\mathbf{k}_q$, the emitted g-momentum, $\mathbf{k}_{g1}$, and the $\bar{q}$-momentum after the emission, $\mathbf{k}_{\bar{q}}$.

This configuration is also shown in Fig. 17.4. The momentum recoils are in this example quite noticeable. In particular they are represented by the angles between the consecutive vectors. *The strong angular condition will require that any new emission must provide a smaller angle than the one characteristic of the emitting dipole.* We now assume that the second gluon is emitted from the dipole between the q and the g_1, see Fig. 17.5.

The directrix is then changed from a triangle to a quadrilateral curve. The strong angular condition corresponds to the coherence requirements on the radiation. The condition will in this case require the second gluon, g_2, to cut off the corner between the q- and the g_1-momentum vectors. We note that these two will recoil (the perimeter of the polygon still corresponds to W!) and the result will evidently lead to a shape with less violent bends.

It is of some interest at this point to consider the other possible color-ordering, i.e. the one which would occur if the same g_2 had been emitted from the dipole between the g_1 and the $\bar{q}$. The corresponding directrix is shown by the heavy broken line in Fig. 17.5. The most noticeable thing is that this color-order produces a directrix which contains sharper corners.

https://doi.org/10.1017/9781009401296.017 Published online by Cambridge University Press

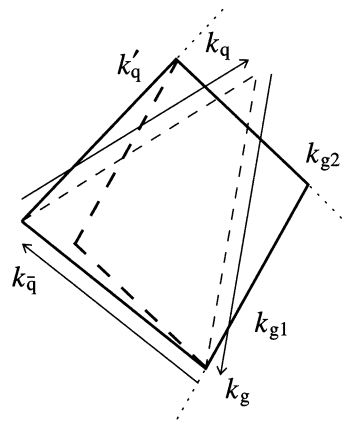

Fig. 17.5. The second gluon emission in the dipole between the q and the g_1 changes the directrix into a quadrilateral.

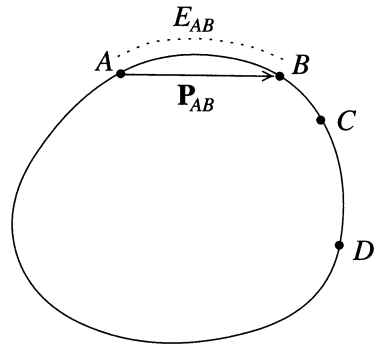

Fig. 17.6. A smooth directrix curve stemming from multigluon emission.

This possibility is not necessarily excluded, because we are working in a three-dimensional space during this emission and the angles are more complex than in a plane. The configuration is, however, in general strongly suppressed as compared to the one with smoother corners.

The characteristic conar angles for the three dipoles are also shown in Fig. 17.5 and they are in general smaller than those obtained after the first emission. It does not take much imagination to understand that *in every new step the strong angular condition will drive some of the new angles towards smaller values, i.e. the directrix curve becomes more and more smoothly bent* as shown in the example in Fig. 17.6. In this case we have

https://doi.org/10.1017/9781009401296.017 Published online by Cambridge University Press

gone over to a continuous curve but it can be considered as emerging from continually smaller gluon emissions as we will show below.

2 A self-similar string directrix

One immediate question is the general structure of the directrix curves we obtain in a cascade containing the coherence conditions of QCD bremsstrahlung. In order to answer this we must be able to make comparisons between different parts of the directrix curves. Such parts correspond to sets of color-connected gluons. The relevant question is whether a group of gluons in one part of the state will look 'similar' to another group somewhere else. To understand the problem we will in particular focus on the regions between the points indicated in Fig. 17.6.

At first sight the two parts AB and CD evidently do not have the same appearance. According to the definition of the directrix the distance along the curve between A and B corresponds to the energy and the vector $\mathbf{AB} \equiv \mathbf{P}_{AB}$ corresponds to the momentum of that part of the directrix. Therefore it is perfectly feasible to go to the rest frame of the region AB and consider the result.

This is the only relevant way to compare different parts of the directrix. In a theory which is Lorentz-covariant we are not interested in differences corresponding to the use of different Lorentz frames nor differences due to rotations of the state within the frames. We will now exhibit some rather puzzling and interesting features of the particular curve drawn in Fig. 17.6, [47].

We can do the same procedure for CD as we have performed for AB. The interesting thing is that the two parts will look exactly alike in their rest frames! Not only that: the original curve is chosen in such a way that the curve itself, the parts AB, CD and any connected part of the curve have the same shape if we consider each in its own rest frame. All parts are *self-similar*. This means that apart from a scale factor and a possible rotation in space they can all be described in the same way:

$$\begin{aligned} A_0(\xi) &= R(2\xi - 3\xi^2 + 2\xi^3) \\ A_1(\xi) &= R(-\xi + 3\xi^2 - 2\xi^3) \\ A_2(\xi) &= R\sqrt{3}(-\xi + \xi^2) \\ A_3(\xi) &= 0 \end{aligned} \tag{17.11}$$

Here, the space part is chosen in the 12-plane and is required to pass through the origin for $\xi = 0$ and $(R, \mathbf{0})$ for $\xi = 1$. The parameter R corresponds to the mass of the state and is the only available parameter for the curve.

The curve in Eq. (17.11) is unique (besides an arbitrary Lorentz trans-

https://doi.org/10.1017/9781009401296.017 Published online by Cambridge University Press

formation) and has the particular property that

$$\dot{A}(\xi_1)\dot{A}(\xi_2) = 6R^2(\xi_1 - \xi_2)^2 \tag{17.12}$$

The reader may convince himself/herself that the results described above are correct by choosing different connected parts, calculating the corresponding boost parameters and considering the emerging function in the rest frame!

The completely self-similar curve in Eq. (17.11) is a limiting case of the following situation. Suppose that we emit a set of gluons in such a way that there is one gluon in the centre at the rapidity $y = 0$ and then symmetrically placed gluons at $\pm n(\Delta y)$ for $n = 1, \ldots, N$, all with the same transverse momentum $k_\perp$. Both the rapidity and the transverse momenta are 'real' variables in the sense that they are measured with respect to a particular axis in the Lorentz frame we are considering.

The color connection will be the obvious one, i.e. from the outermost parton at $N\Delta y$ to $(N-1)\Delta y$ etc., ending on the gluon at $-N\Delta y$. We will assume that the two at the endpoints are the q and the $\bar{q}$ for an open string.

This means that the nth gluon (we will allow n to take both positive and negative values) will have energy and momentum equal to

$$\begin{aligned} e_n &= k_t \cosh(n\Delta y) \\ k_{1n} &= k_t \\ k_{2n} &= k_t \sinh(n\Delta y) \end{aligned} \tag{17.13}$$

We are obviously not describing the state in the cms. Nevertheless, this particular state will on a local level look exactly the same (almost) everywhere because the mass of a neighboring group of gluons is always

$$\begin{aligned} M_2^2 &= 2k_t^2[\cosh(\Delta y) - 1] \\ M_3^2 &= 2M_2^2 + 2k_t^2[\cosh(2\Delta y) - 1] \end{aligned} \tag{17.14}$$

etc. with the lower index corresponding to the number of neighbors counted.

The total energy of the state is easy to sum up:

$$E = k_t \frac{\sinh[\Delta y(2N+1)/2]}{\sinh(\Delta y/2)} \tag{17.15}$$

and correspondingly the momentum is $P_1 = (2N+1)k_t$ along the 1-axis. We may then boost the state by the velocity P_1/E to the cms.

We now consider the case when $N \to \infty$ and $\Delta y \to 0$ in such a way that the product $N\Delta y \to \beta$. Then we obtain for the derivative of the directrix

https://doi.org/10.1017/9781009401296.017 Published online by Cambridge University Press

function with respect to ξ, where $\xi = (N - n)/(2N)$,

$$\begin{aligned}
\dot{A}_0 &= k_\perp \frac{\sinh\beta\cosh[(1-2\xi)\beta] - \beta}{\sqrt{\sinh^2\beta - \beta^2}} \\
\dot{A}_1 &= k_\perp \frac{\sinh\beta - \beta\cosh[(1-2\xi)\beta]}{\sqrt{\sinh^2\beta - \beta^2}} \\
\dot{A}_2 &= k_\perp \sinh[(1-2\xi)\beta]
\end{aligned} \tag{17.16}$$

We also note that ξ, defined in this way, always fulfils $0 \leq \xi \leq 1$. In this way we obtain a set of possible directrix functions containing two shape parameters, k_t and β. It is easy to integrate Eqs. (17.16) but we will leave that for the interested reader.

Instead we consider the limit when $\beta \to 0$ and $k_t \to \infty$ so that $k_t\beta \to R\sqrt{3}$. Then it is easy to prove that the vector in Eq. (17.16) will approach the derivative $\dot{A}$ of Eq. (17.11) at every point ξ.

The states we have introduced in this way seem to be unusual in the sense that the gluons all have the same local properties, in particular they all have the same value of the transverse momentum variable k_t. It is instructive to notice that this value of the transverse momentum is not equal to the invariant transverse momentum we would use to order the emissions in the dipole cascade model.

Thus we obtain for the invariant transverse momentum (Eqs. (16.39) and (17.14)):

$$k_\perp^2 = \frac{M_2^4}{M_3^2} = \frac{2k_t^2\sinh^2(\Delta y/2)}{1 + 2\cosh^2(\Delta y/2)} \tag{17.17}$$

In order to understand that such a state actually can come out of a cascade we note that we may start with a situation where the original q and $\bar{q}$ are in some frame going out with rapidities $\pm N\Delta y$ and the same transverse momentum k_{t1}. This means that the total squared mass of the system is $s = 2k_{t1}^2[\cosh(2N\Delta y) - 1]$. Next we emit a gluon with the invariant $k_{\perp 1}$ at the invariant rapidity $y = 0$. The rapidity condition means that the two emerging dipoles are exactly equal. This means that we can find a new frame with the q, g_1 and $\bar{q}$ moving at rapidities $\pm N\Delta y$ and 0 in that frame. We define $k_{\perp 1}$ so that all the three partons have the same transverse momentum, k_{t2}, in that new frame.

To determine the variables it is only necessary, due to the symmetry, to conserve the total mass:

$$\begin{aligned}
s &= 2k_{t1}^2[\cosh(2N\Delta y) - 1] \\
&= 2k_{t2}^2[(\cosh(2N\Delta y) - 1] + 2[\cosh(N\Delta y) - 1)]
\end{aligned} \tag{17.18}$$

This provides an equation that determines k_{t2} in terms of Δy and k_{t1}. The

https://doi.org/10.1017/9781009401296.017 Published online by Cambridge University Press

invariant $k_{\perp 1}$ is given by

$$k_{\perp 1}^2 = \frac{s_{qg_1} s_{g_1\bar{q}}}{s} = k_{t2}^2 \frac{2\sinh^2(N\Delta y/2)}{2\cosh^2(N\Delta y/2)+1} \tag{17.19}$$

and we recognise this for $N = 1$ from Eq. (17.17).

In the next step we divide each of the dipoles qg_1 and $g_1\bar{q}$ in the middle and again go to a new frame in which the q and $\bar{q}$ have rapidities $\pm N\Delta y$, the two new gluons have rapidities $\pm N/2\Delta y$ and the original gluon still goes out at $y = 0$, all with transverse momenta k_{t3}. Again it is, due to symmetry, only necessary to fulfil the total squared mass condition:

$$\begin{aligned} s = 2k_{t3}^2 \{&[\cosh(2N\Delta y_3) - 1] + 2[\cosh(3N/2\Delta y_3) - 1] \\ &+3[\cosh(N\Delta y_2) - 1] + 4[\cosh(N/2\Delta y_2) - 1]\} \end{aligned} \tag{17.20}$$

This condition will fix k_{t3} in terms of the earlier k_t-variables. We can evidently continue this process every time choosing the Δy-variables to be the same at each level and filling in more and more gluons. The k_t- and the invariant $k_\perp$-variables will quickly decrease because of the number of terms in the mass condition.

The ordinary cascade states contain many more irregularities. It is, however, a fact that most of the fluctuations in the cascade states are connected to the first two gluon emissions. We will discuss this result, [12], in Chapter 18 after we have developed more analytical tools.

17.7 Single-parton emission compared to the DCM procedure

1 The splitting formulas

We start with a partitioning of the dipole radiation formulas, Eq. (17.2), into two parts, each corresponding to the contribution from one of the charges. In section 16.4 we have derived the strong angular ordering condition, which is one way to include the coherence conditions in QCD bremsstrahlung. Then the dipole emission region is divided into two parts, according to the angle with respect to the existing partons. Although the formula in Eq. (16.47) is a good approximation to the cross section for soft gluon emission it is necessary, for hard and collinear gluon emissions, to account for the contributions from the polarisation correlations in the numerator of the cross section. It is therefore necessary to provide more precise expressions.

We assume that the gluon (index 2) is, in connection with the first formula in Eq. (17.2) emitted close to the q-particle (index 1). Then the squared mass $s(1 - x_3) = s_{12} \equiv Q^2$ is small and Q is usually referred to as the virtual mass of the qg-pair. The reason is that intuitively we may

https://doi.org/10.1017/9781009401296.017 Published online by Cambridge University Press

consider the process as being in two steps: firstly there is the production of an off-shell q (with positive mass Q corresponding to a time like vector); secondly this then decays into the on-shell qg-pair, see Fig. 16.2 (note the discussion in the corresponding text that such a statement is not gauge-independent and that therefore one must be careful).

Also, $x_3 \to 1$, i.e. the $\overline{q}$ takes energy $\simeq \sqrt{s}/2$. The q and g will together take $x_1 + x_2 \simeq 1$ of the remaining energy $\sqrt{s}/2$. We may then write the bremsstrahlung formula in the first line of Eq. (17.2) as the product of a factor corresponding to the production of Q^2 and another factor, *the splitting function* $\mathscr{P}^q_g(z)$ for the virtual q to emit the g with g-fraction $z = x_2$:

$$\begin{aligned} dn_g &= \frac{\alpha_s}{4\pi}\frac{dQ^2}{Q^2}\mathscr{P}^q_g \\ \mathscr{P}^q_g &= \frac{4}{3}\frac{[1+(1-z)^2]}{z} \end{aligned} \tag{17.21}$$

The corresponding splitting function for the (virtual) q to emit the on-shell q with fraction $z = x_1$, $\mathscr{P}^q_q(z)$, evidently becomes

$$\mathscr{P}^q_q = \frac{4}{3}\left(\frac{1+z^2}{1-z}\right) \tag{17.22}$$

In order to exhibit the polarisation contributions in the numerator of the formulas in Eqs. (17.2) and (17.21), (17.22) we will derive the results from the Rutherford scattering formula we obtained in Eq. (5.40). We consider the scattering of two (massless) spin 1/2 particles in the cms, described initially by the vectors $p_{1,2} = (W/2, \pm W/2, \mathbf{0}_\perp)$, with momentum transfer q to final states $p_{3,4} = (W/2, \pm p_\ell, \pm \mathbf{p}_\perp)$. We will then have the kinematical relations (in terms of the scattering angle θ)

$$\begin{aligned} p_\ell &= \frac{W\cos\theta}{2}, \quad p_\perp^2 = \frac{W^2\sin^2\theta}{4} \\ q &= \left(0, \frac{W(1-\cos\theta)}{2}, -\mathbf{p}_\perp\right) \end{aligned} \tag{17.23}$$

If we define the splitting variable z at the vertex $p_1 \to q p_3$ by the lightcone fraction $q_0 + q_\ell = z(p_{01} + p_{\ell 1})$ (note that this means that

$$1 - z = (p_{03} + p_{\ell 3})/(p_{01} + p_{\ell 1}) = (1 + \cos\theta)/2)$$

then we obtain for the variables in Eq. (5.40)

$$s = \hat{s} = W^2, \quad p_\perp^2 = z(1-z)s, \quad Q^2 = -q^2 = zs \tag{17.24}$$

We then obtain from the Rutherford scattering cross section (remember that the fine structure constant α becomes in QCD $C\alpha_s/2$, with C a color

https://doi.org/10.1017/9781009401296.017 Published online by Cambridge University Press

factor and α_s the coupling):

$$d\sigma = 2\pi \left(\frac{4\pi\alpha_s}{3s}\right) \frac{\alpha_s dQ^2}{4\pi Q^2} \mathscr{P}_g^q \tag{17.25}$$

i.e. we obtain the two factors mentioned above corresponding to the production of the (virtual) Q^2 multiplied by the splitting $q \to q, g$. We note that in this case we start with an on-shell (massless) q, which splits into another massless q and a spacelike gluon propagator $Q^2 = -q^2$. Any splitting process must bring (at least one of) the final-state particles to a smaller (or spacelike) mass and we will come back to this in the treatment of deep inelastic scattering in Chapters 19 and 20.

The first factor in Eq. (17.25) stems from the azimuthal angular (in)dependence and the second has the intuitive meaning of the interaction cross section for two waves with (longitudinal) wavelengths $\simeq 1/\sqrt{s}$ and interaction constant $C\alpha_s$ (or, if we go back to the derivation of the Rutherford formula in Eq. (5.40), we find $1/s$ as the 'flux factor' from the incoming state).

We may consider along the same lines the process $g \to q\bar{q}$ from Eq. (5.41), which in field theoretical language corresponds to the crossing-symmetric result of Rutherford scattering. It is straightforward to see that we obtain the splitting functions $\mathscr{P}_q^g$ and $\mathscr{P}_{\bar{q}}^g$ as

$$\mathscr{P}_q^g = \mathscr{P}_{\bar{q}}^g \quad \propto \quad z^2 + (1-z)^2 \tag{17.26}$$

(note that, although the process must be symmetric, in this case there will be no z- or $(1-z)$-pole! We have discussed this in connection with the properties of the polarisation function in QCD, section 4.5. It stems from helicity conservation and we will return to the implications in the next subsection). The normalisation is discussed in Eq. (17.35).

Along the same lines one can derive, [5], the splitting function for a $g \to gg$ process:

$$\mathscr{P}_g^g(z) = 3\left[\frac{1-z}{z} + \frac{z}{1-z} + z(1-z)\right] \tag{17.27}$$

It is important to clarify the notion of virtual mass. Consider the decay situation described in Fig. 17.7. One particle with energy-momentum vector (in lightcone coordinates along its direction of motion) $Q = (W_+, W_-, \mathbf{0}_t)$ decays into two, which share the positive lightcone component in the fractions z and $1-z$ and have transverse momenta $\pm\mathbf{k}_t$. If we assume that the decay products are massless then we obtain immediately for their energy-momenta

$$\left(zW_+, \frac{\mathbf{k}_t^2}{zW_+}, \mathbf{k}_t\right) \quad \text{and} \quad \left((1-z)W_+, \frac{\mathbf{k}_t^2}{(1-z)W_+}, -\mathbf{k}_t\right) \tag{17.28}$$

https://doi.org/10.1017/9781009401296.017 Published online by Cambridge University Press

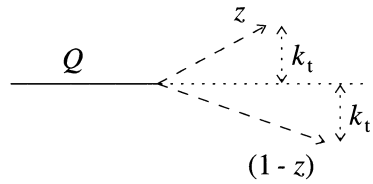

Fig. 17.7. The decay of a particle with mass Q into two particles with compensating transverse momenta and fractions z and $1-z$ of the lightcone component of the mother particle.

Energy-momentum conservation then means that

$$W_- = \frac{\mathbf{k}_t^2}{zW_+} + \frac{\mathbf{k}_t^2}{(1-z)W_+} \tag{17.29}$$

which implies that

$$Q^2 \equiv W_+W_- = \frac{\mathbf{k}_t^2}{z(1-z)} \tag{17.30}$$

If the decay-product mass-squares are known to be Q_1^2, Q_2^2 then $\mathbf{k}_t^2 \to \mathbf{k}_t^2 + (1-z)Q_1^2 + zQ_2^2$ in Eq. (17.30).

The relationship in Eq. (17.30) means that the mass parameter Q is proportional to the transverse momentum. The proportionality factor depends upon the fractional partitioning in energy-momentum. Different authors have used different definitions of z and of k_t and this changes the relationship a bit. But it is anyhow evident that

- it is possible to calculate this 'virtual mass' of the decaying particle from the decay products, whether we know x_1 and x_3 (in the DCM and ARIADNE) or z and k_t, or equivalent variables (in the Webber-Marchesini HERWIG and Sjöstrand's JETSET);
- the relationship between the virtual mass and the transverse momentum means that in general both of them will diminish in a similar way as the cascade proceeds downwards and that they can both be used as ordering variable.

We will see in the next subsection that if the stochastic process contains two or more competing subprocesses then the choice of ordering variable does play a role and may lead to different physical results.

We end by describing the reasons for choosing the numerator polarisation sums in Eq. (17.2) with these particular powers for the q- and g-emissions.

There are two features which are necessary to understand in connection with these choices, i.e. the power 3 for a gluon and the power 2 for a quark (antiquark) emitter:

- outside the collinear situations the numerator is a slowly varying function and there is no clear indication of the way one should choose the interpolation between the pole-dominated regions.
- all formulas should be arranged so that there is no double-counting in the cross sections.

The formulas are derived in such a way that they will fulfil these two requirements, i.e. exhibit the right splitting function structure at the pole and correspond to a smooth interpolation away from it. To see this assume that we have an emission which is collinear to an already emitted gluon. This means that we consider the situation when $x_3 \to 1$ and so $1 - x_1 = z$, i.e. the splitting variable. Then the result for a gluon emission cross section in Eq. (17.2) is

$$\frac{1 + (1-z)^3}{z} \tag{17.31}$$

Together with the corresponding factor from the adjoining dipole (obtained by putting z equal to $1 - z$ we then have

$$\frac{1 + (1-z)^3}{z} + \frac{1 + z^3}{1 - z} \quad \propto \quad \left[\frac{z}{1-z} + \frac{1-z}{z} + z(1-z)\right] \tag{17.32}$$

which is just the right Altarelli-Parisi splitting function (apart from a color factor), cf. Eq. (17.27).

2 *The gluon splitting process*

Up to now we have only been concerned with the emission of new gluons. There is in QCD also the process of gluon splitting, i.e. when a gluon decays into a quark-antiquark pair $g \to q\bar{q}$. This is a rather small correction but it is of large interest when the experimentalists are able to provide precise data on the appearance of heavy quarks in the centre of phase space. We will follow [10] in this description.

We have already mentioned before that e.g. charm and bottom flavors are so heavy that they cannot be produced in a soft fragmentation situation. They can, however, be produced 'immediately', i.e. as first pairs in an e^+e^- annihilation event when we have passed the mass threshold $2M_Q$ with M_Q the heavy quark mass. In that case they will for large energies end up in final-state particles with large rapidities. *They can, however, also be produced from the gluon splitting process and this is the only possible source for small rapidities.*

https://doi.org/10.1017/9781009401296.017 Published online by Cambridge University Press

Just as in connection with the emission of a second gluon in the cascade in Eq. (17.1) there has been an explicit formula derived, [56], for the process $e^+e^- \to qQ\bar{Q}\bar{q}$, where we use the symbol $Q\bar{Q}$ for a second quark-antiquark pair. If we use the indices 1–4 for the particles as they are written in the production description then the exact (rather long and involved) formula simplifies as follows:

$$\frac{d^4\sigma}{dx_1 dx_4 ds_{23} dz} \sim \frac{x_1^2 + x_4^2}{(1-x_1)(1-x_4)} \frac{z^2 + (1-z)^2}{s_{23}} \tag{17.33}$$

This approximation is valid when the original pair has cms energy fractions x_1 and x_4 which are not too small and the mass square s_{23} of the extra $Q\bar{Q}$-pair is not large. Finally the variable z is the lightcone fraction of the energy-momentum of the $Q\bar{Q}$-pair which is carried by the particle indexed 2 and the expression is of course symmetric between z and $1-z$.

This expression is factorisable and can be understood as follows:

- There is a first emission of a gluon (23) from the original $q\bar{q}$-pair (at the end indexed 14) with the cross section in Eq. (17.2).
- There is after that a splitting of the gluon into the pair 2 and 3 with a cross section

$$\simeq \frac{n_f \alpha_s}{4\pi} \frac{dQ^2}{Q^2} [z^2 + (1-z)^2] dz \tag{17.34}$$

In Eq. (17.34) we have used the conventional variables, the virtuality Q^2 and the fractional energy-momentum-sharing variable z. We also note the appearance of a factor n_f for the number of flavors that can be produced. The expression

$$\mathscr{P}_q^g = n_f [z^2 + (1-z)^2] \tag{17.35}$$

is usually referred to as the splitting function for $g \to q\bar{q}$ and it occurs in that form in the QCD single-parton cascades.

It is useful to try to compensate for some of the approximations in the derivation of Eq. (17.33) by choosing the kinematical variables with care. We will not go into details; they can be found in the original paper, [10], for ARIADNE and there are corresponding choices for the JETSET and the HERWIG Monte Carlo simulation programs.

There are two interesting features about the gluon splitting process.

- There is only the virtuality pole in Eq. (17.34). If we compare with the splitting formulas we derived above in subsection 1 we note that both the processes $q \to qg$ and $g \to gg$ also have poles in the z-variable. This is the major reason why the gluon splitting process is much smaller than the other two.

https://doi.org/10.1017/9781009401296.017 Published online by Cambridge University Press

- When we introduce the gluon splitting together with the gluon emission process there will be competition between the possibilities that a particular dipole will emit a new gluon or that one of the already produced gluons between two dipoles is split up into a $q\bar{q}$-pair.

In ARIADNE the choice has been to partition the cross section for gluon splitting equally between the two dipoles connected to a particular gluon (this is the reason why there is a factor of 2 in front in the expression in Eq. (17.34)). There is nothing fundamental about this but we have checked that it is a good approximation to the precise matrix element almost everywhere in the phase space.

The competition between the two processes means that now the Sudakov factor in Eq. (17.4) will contain two (three) contributions for each qg- or $g\bar{q}$- (gg-) dipole, one for the emission of a further gluon and one for the splitting up of the gluon(s) at the corners. *And now the ordering variable becomes interesting.* We have already seen that the virtuality, Q^2, is related to the squared transverse momentum by Eq. (17.30).

But, due to the occurrence of the denominator $z(1-z)$ in Eq. (17.30), a given (large) Q^2 can be obtained either from the situation when we have a large $k_\perp^2$ and a value of $z \sim 1/2$ or from a small value of $k_\perp^2$ and a $z \sim 1$ or $z \sim 0$. Thus if we order in Q^2 we would be comparing soft and/or collinear gluon emission to hard, i.e. large $k_\perp^2$, emission of a $Q\bar{Q}$-pair.

The major result of [10] is that if we want to use Q^2 as the ordering variable (which is done in the JETSET cascade) rather than $k_\perp^2$ as ordering variable (for the precise definition of this variable consider [10]) one obtains at least a factor of 2, sometimes 3–5, fewer gluon splitting pairs.

We are, however, talking about a change from about 5%–8% ($k_\perp$-ordering) to about 2% (Q^2-ordering) when comparing gluon splitting into $q\bar{q}$-pairs to gluon emission into 'new' gluons. But it is of large interest as it is the only known mechanism that provides heavy flavors in the centre of phase space. In the case of gluon splitting into a $Q\bar{Q}$-pair, then the final state is treated in the Lund model as two independent strings, one from a 'forward' q to the $\bar{Q}$ and one from the Q to a 'backward' $\bar{q}$. This means that after a splitting the remaining string mass(es) may be very much reduced, implying effectively that further radiation is correspondingly reduced.

3 *Single-parton coherent cascades*

The splitting functions correspond to *collinear approximations to the radiation cross sections.* They are correct when the emitted parton is sufficiently close to the original parton. However they can be more or less good approximations when the gluon is further away. The results depend upon the definitions of the kinematical variables used.

https://doi.org/10.1017/9781009401296.017 Published online by Cambridge University Press

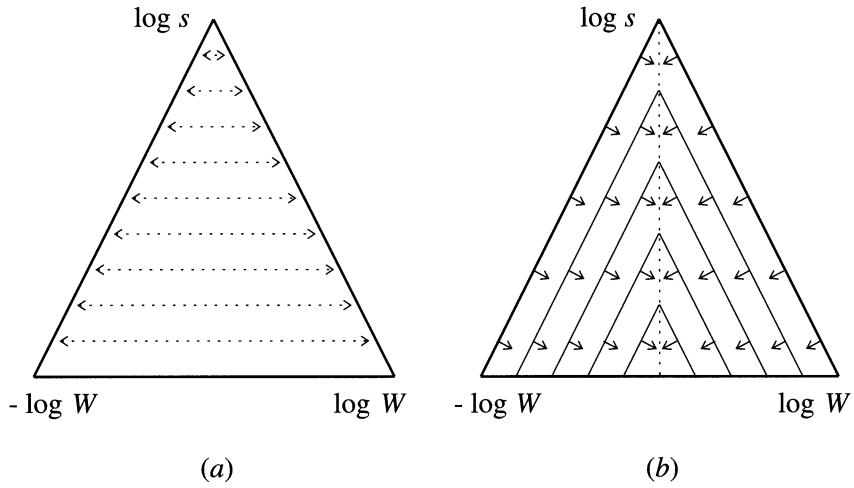

Fig. 17.8. The triangular phase space for gluon emission with arrows showing the ways (*a*) HERWIG and (*b*) JETSET search it to find the possible parton emissions. HERWIG goes sideways in an angle or rapidity variable, all the time looking upwards and downwards at all $k_\perp$ allowed for that rapidity. JETSET orders in Q^2: the thin solid lines corresponds to fixed Q^2, and are investigating different values of z (left-hand side) or $1 - z$ (right-hand side).

We will in this subsection consider two different ways to implement the concept of a single-parton cascade, i.e. when each already emitted parton is independently allowed to continue to radiate new partons in a branching process. We have shown in Chapter 16 that in the mean, i.e. for inclusive distributions, one may, by imposing the strong angular ordering condition, obtain correct results at least in the collinear limit.

It is evident that, whichever model one uses the same phase space is around with respect to further emissions. In this book we have used a phase-space description relevant to the DCM in terms of a triangle in $\kappa = \log k_\perp^2$ and y. We show it again in Fig. 17.8 this time in order to exhibit the ways in which HERWIG, [94], and JETSET, [105], include the phase-space restrictions.

We have already said that in ARIADNE and the DCM the ordering variable is κ, i.e. one starts at the largest available $k_\perp$ and then proceeds downwards in the triangle all the time looking, via the Sudakov factor, in the allowed rapidity regions for new emissions.

A HERWIG cascade can be easily traced in the DCM triangle. In HERWIG the authors use as ordering variable the angle θ with respect to some axis, chosen at random. Remembering the relation between angle

https://doi.org/10.1017/9781009401296.017 Published online by Cambridge University Press

and (pseudo)rapidity, y,

$$y = \log[\cot(\theta/2)] \simeq -\log(\theta/2) \tag{17.36}$$

this means that they are not going downwards in phase space, they are instead going sideways in the original triangle, *thereby obviously fulfilling the strong angular ordering condition for coherence in the QCD bremsstrahlung*. They further use the variable $\xi = E\theta \sim k_\perp$, which in general is a good approximation to the relation between the energy and transverse momentum of the emitted parton.

The HERWIG authors arrange it in the same way but in the opposite direction, i.e. towards the $\bar{q}$-end with the obvious exchange $\theta \to \pi - \theta$. Again they continue towards smaller angular variables, i.e. towards larger rapidities in that direction. The argument in the splitting functions and the running coupling constant is ξ.

Though it is obviously opposite to the arrangement in the DCM, one can just as well sample the possible jets by going sideways and looking up and down as going downwards and looking right and left. Any time a jet is found for some value of (θ, ξ) it is implemented as a fold like those drawn out of the original triangle in Chapter 15. Then this jet region, i.e. the triangular fold, is searched through in the same way and subtriangles, i.e. subjets, are noted and followed up, etc.

At the end all the emitted partons have been sampled and all the precise kinematical variables have been calculated. Although the choice of energies and angles does not give us bona fide Lorentz-covariant variables the process works very well and seems to give results very close to those of the DCM. We will come back shortly to the Webber cluster fragmentation model, which is used at the end to provide final-state hadrons.

Before that we will briefly consider the way the cascade is implemented in Sjöstrand's JETSET. There the variables Q^2 and z are defined by means of Lorentz invariants. For the precise choices we refer to the original papers, [105]. This means, however, a different way of searching through the triangular region. The process corresponds to passing inwards towards the centre of the triangle from both sides; one of the sides corresponds essentially to using z as the positive lightcone energy-momentum fraction and the other to the negative lightcone fraction. From the relationship in Eq. (17.30) it is evident that if we identify the triangle variables $\kappa \sim \log Q^2 + y_z$ and $y \sim y_z$ then using on one side $y_z = \log(z/2)$ and on the other side $y_z = \log(1-z)/2$ provides a mapping.

It is necessary to calculate the available phase space in z for a given Q^2 etc., but all this is done in a very effective way in the Monte Carlo routines. Once again the background triangle is searched through and every time a parton emission occurs then it is accepted as long as the correct angular ordering condition is fulfilled. Then afterwards this new fold is searched

through along the same lines to obtain subfolds, which again are searched through, etc.

There is some possible bias in this procedure of checking the angular ordering afterwards, [70]. There are, however, to our present knowledge no observable consequences of such a bias. It should also be remarked that as the final fragmentation is done by means of the Lund model string scenario the suggested process is not only infrared stable but the possible errors may become hidden. It is known that some earlier, even rather gross, violations of the strong angular conditions in the partonic cascade can be overcome by imposing string fragmentation.

4 *The Webber cluster decay model for fragmentation*

We will end this section with a discussion of the Webber fragmentation model, [110]. The basic idea is to continue the cascade to a certain level and then to let all remaining gluons decay into $q\bar{q}$-pairs. The final state is then sampled to ensure that it will be composed from (color-singlet) clusters stemming from a q from one gluon and a $\bar{q}$ from a color-adjacent gluon.

The way to implement this is to provide the gluons with a fictitious mass m_g so that below a certain virtuality there is no longer any possibility left of emitting more gluons. All the available gluons should then split up into lower-mass $q\bar{q}$-pairs. In practice it is sometimes necessary to force this breakup. In this way there will be a set of clusters, containing the energy-momentum of the (color-)adjacently produced q and $\bar{q}$.

This is similar to the Lund model prescription but there is no requirement that the clusters should have a fixed mass. Instead there will be, as in the Artru-Menessier-Bowler model, a continuous mass spectrum. This time there is a lower cutoff but it does happen frequently that some of the clusters will attain large masses.

The next step is to let the clusters decay into two-particle states, conserving all quantum numbers and only using phase space and The Particle Data Group tables. In practice it is necessary to work hard, just as Sjöstrand has done in connection with the JETSET fragmentation routines, to decide upon the branching ratios that are relevant for different decay channels. There are three practical problems in this program (even after any amount of hard work), W1–W3 as follows.

W1 The large-mass clusters cannot be allowed to decay isotropically into two-particle states, because there will then be much too much transverse momentum generated. This is solved by using a string-breaking routine (which works to cut up the clusters longitudinally, i.e. along the color-connected gluon directions) so that the large

https://doi.org/10.1017/9781009401296.017 Published online by Cambridge University Press

masses are brought down below a certain level to where the method works.

The reason to choose a string-breaking routine is that in this way the final states are not distorted from the cascade distributions, which fulfil the strong angular conditions. The large-mass states typically stem from situations in which there are one or more collinear partons going along the original q-direction, and likewise a few along the $\bar{q}$-direction with little gluonic activity in between. These are the states, usually called two-jet states, which in the Lund model would be similar to the original $(1 + 1)$-dimensional string breakup situation. If all the transverse momentum (with respect to some chosen observed axis) stems from the cluster decays then it is necessary to 'tune' the cluster sizes in order to be able to account for the 'gaussian' fluctuations which are introduced in the Lund model.

W2 The requirement that the clusters should decay into just two final-state hadrons means that there are hardly any hadrons with a value of the fragmentation variable $z \sim 1$. The energy sharing will effectively damp large rapidity values for the decay products.

This is solved by introducing a certain number of single-particle clusters, together with a procedure to rearrange the corresponding cluster energies 'backwards', i.e. towards the neighboring 'ordinary' clusters.

W3 The straightforward application of a cluster decay to baryon-antibaryon production means that the B and $\bar{B}$ in a pair stem from the same cluster. The property that the observed $B\bar{B}$-pairs seem to be dragged apart longitudinally, i.e. in the Lund model along the string direction, and also the (lack of) correlations in the transverse momentum of the pair mean that this cannot be the major source of such production.

This is solved by allowing some of the gluons to split up into diquark-antidiquark pairs thereby producing clusters with baryon and antibaryon quantum numbers. By a reasonable choice of the number and kinematics of such breakups one obtains a good description of the observed baryon and antibaryon distributions. But there seems to be a set of similar problems as in the Lund model in describing the baryon resonances, in particular the baryons with strangeness.

The final result of the fragmentation routines is in most cases indistinguishable from the results of the Lund model and both models certainly are well in agreement with most parts of the present experimental data.

17.8 Some further comments

1 The recoil and color-interference problems

In this subsection we will treat some particular problems connected with the approximations which are made in the partonic cascades. We will be satisfied to investigate these problems within the DCM, where there has been an extensive investigation. There are problems of three different kinds:

1 the *recoil problems* along the cascade;

2 the relationship between the exact result from the second-order perturbative QCD results (which we will henceforth refer to as PQCD2) and the cascade results;

3 the quantum mechanical color-interference effects, which occur in the PQCD2, but are neglected in the cascades.

We start with the recoil problems. There are two kinds of recoil problem. There is firstly the loss of energy of the emitters and there is secondly the necessary momentum compensation. The energy loss corresponds to the obvious requirement that all the fractional cms energies after the emission fulfil $x_j < 1$. Further the relative angles between the partons after the emission are also defined by the x_j's. To see this we note that

$$s_{12} = s(1 - x_3) = 2E_1E_2(1 - \cos\theta_{12}) \quad \Rightarrow \quad \sin^2\left(\frac{\theta_{12}}{2}\right) = \frac{1 - x_3}{x_1x_2} \tag{17.37}$$

But *the relative angles between the original dipole and the final state* are not defined in this way. We have already mentioned that according to the transition matrix element they are given by the overlap of the original and final currents. This results in an angular correlation factor $1 + \cos^2\theta$ with θ the angle between the directions of the initial-state e^+e^- annihilation current and the produced $q\bar{q}$-current.

The current in a $qg\bar{q}$-state is more complex; there is nevertheless a preferred direction in the final state, which can be most easily described as the axis with a minimum for the transverse momentum combination $k_{\perp 1}^2 + k_{\perp 3}^2$ with respect to the dipole axis. This means that the q- and $\bar{q}$-charges try to keep as much as possible to their original directions.

There is a prescription given by Kleiss, [85], of how to implement this correlation in a Monte Carlo generation and we refer to this original paper for the details. There is, however, no known prescription for the alignment between the final state and the original dipole direction when the emitters are gg-, qg- or $g\bar{q}$- pairs.

https://doi.org/10.1017/9781009401296.017 Published online by Cambridge University Press

Some guidance can be obtained from the PQCD2 results for the last two cases. In [103] a comparison is made between the full PQCD2 and the Monte Carlo implementation of the DCM in ARIADNE.

The results are that ARIADNE with the ordering variable $k_\perp$ works very well over the whole phase space even when the transverse momentum $k_{\perp 1} \simeq k_{\perp 2}$, i.e. when the first and the second gluons have almost the same hardness. In that paper several different recoil strategies are investigated. Owing to the large amount of 'noise' from the multiparton distributions in the final state and the subsequent fragmentation into hadrons it is not possible to discern the differences between the different recoil schemes.

In the same paper the color-interference term between different color-flow situations has also been investigated. We have already mentioned this problem (see Chapter 15). It is by no means clear that a theory which only contains the production mechanism for the charges, as perturbative QCD does, is not neglecting some structure related to the fields themselves. The color-interference term turns out to be negative and therefore it is not easily introduced into any probabilistic scheme like a Monte Carlo simulation program. It is, however, possible to disentangle the effect so that the PQCD2 formula can be subdivided into two gauge invariant terms:

$$d\sigma \propto B_1 - \frac{B_2}{N_c^2} \tag{17.38}$$

where B_1 and B_2 are positive and N_c is the number of colors.

Intuitively B_2 corresponds, just as in Eq. (17.1), to the contribution from the $q\bar{q}$-dipole, which is recoiling with respect to the gluon that is firstly emitted. Therefore the term B_2 is large when the second gluon is oppositely directed to the first, while it is small when the two gluons go in the same hemisphere. Nevertheless the color-interference term is only of the order of 10% compared to the other contribution.

The possibility of measuring the existence of such a color-interference factor is of obvious interest. In [103] the method is to use ARIADNE to generate multigluon events and to stop the generation after the emission of two gluons. Then the result is corrected by a weighting factor between the full second-order matrix element and the ARIADNE probability, with and without taking the color-interference term into account.

Then the cascade is continued, the final state fragmented into hadrons and different configurations investigated. It is found that there is an effect of the order of 10% between just the two configurations mentioned above, i.e. when there are two jets in the same hemisphere and two jets in opposite hemispheres with respect to the thrust axis. For the necessary experimental cuts and the necessary statistics to find the effect we refer to the original paper.

2 A moving interface between the dipole cascade and the Lund fragmentation

We have noted that the dipoles in the dipole cascade model are spanned between the gluons in the same way as the segments of a Lund string (with the Lund interpretation of a gluon as an internal excitation on the string). Therefore in the Lund model further gluon emission in the DCM corresponds to excitations on an already existing string segment.

In accordance with our considerations in Chapter 15 this implies that a straight string segment will be bent and a region of the string surface which originally was spanned between two lightcone directions will after the new emission still be spanned between them but now via a third lightcone direction. The new excitation is, however, in general much smaller than the earlier ones. We will show that by explicit calculations on the mean cascade development in Chapter 18.

From the investigation of how gluon emissions will affect the directrix, section (17.6), we concluded that, for a given directrix, subsequent gluon emission tends to smooth out the sharp corners stemming from the first few excitations. The pole structure of the emission cross section means that most gluons will be collinear or soft as compared with the emitters.

Therefore these further emissions do not really change the general shape very much, although they may correspond to some increase in the total generalised phase space, i.e. the λ-measure we have introduced before. A natural question is to what extent it is possible to differentiate between the results of such multigluon emission and the final-state fragmentation process. In other words, is there some particular scale where the effects of the fragmentation takes over from the the dipole cascade?

We will use the results of [12] to answer this question. The softer gluons turn out to correspond to a noise of the same kind as the fragmentation process. They increase the multiplicity and the transverse momentum fluctuations. But it is possible to compensate these effects by changing the fragmentation parameters in the Lund fragmentation model in such a way that all inclusive event observables are the same independently of where we stop the cascade.

This is true at least if we use a cascade stop at $k_{\perp,c}$ with $k_{\perp,c} = 7$ GeV or any number below that (but above Λ_{QCD}). In this way we obtain a functional dependence on $k_{\perp,c}$ of the main fragmentation parameters, a and b in the fragmentation function and σ corresponding to the width in the zero-point transverse momentum fluctuations.

The result is shown in Fig. 17.9 and we conclude that while a and σ need small adjustments it is necessary to change b appreciably with $k_{\perp c}$. It is particularly interesting to see that the value of a deduced in this way tends to be stable a bit above 0.5, i.e. it is close to the value of the ρ-Regge

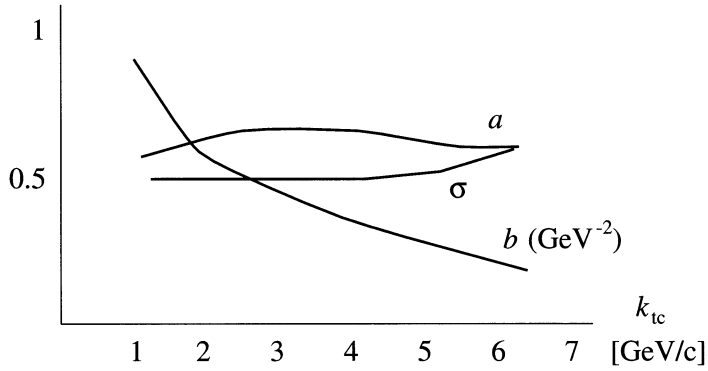

Fig. 17.9. The dependence of the parameters a, b and σ on the cutoff in $k_{\perp c}$ for the cascade.

intercept. This is in accordance with the interpretation we obtained from the discussion in Chapter 10. The parameter σ governing the transverse momentum fluctuations increases by around 25% from small cutoff values to the larger ones.

We have related the parameter b to the transverse width of the string in Chapter 11 and also, via the relation $b\kappa \sim \alpha_s/12$, to the coupling α_s. We find that b decreases from around 0.85 at $k_{\perp,c} = 1$ GeV to 0.15 at $k_{\perp,c} = 7$ GeV. This is just what we would expect from the interpretation that b is proportional to the inverse logarithm of $k^2_{\perp c}$, i.e. to the running QCD coupling.

If we continue downwards in the cascade we resolve the string better and better in transverse momentum. But this means that the string is less and less well resolved in the canonically conjugate space, i.e. in impact parameter space. Therefore we should expect that the transverse width of the string becomes larger and thus also the value of b. Using the value of the running coupling constant derived in Chapter 4 as a function of $k_{\perp,c}$ we obtain a reasonable agreement with the formula above for $\kappa \simeq 0.2$ GeV^2 although we need a somewhat large value of $\Lambda_{QCD} \sim 0.4$–0.5 GeV.

The main point is that in this way there is a moving interface between the fragmentation process and the dipole cascade in the Lund model. The model is very stable, in particular infrared stable.

https://doi.org/10.1017/9781009401296.017 Published online by Cambridge University Press